Spring 4-2012

PP and CNO-Cycle Nucleosynthesis: Kinetics and Numerical Modeling of Competitive Fusion Processes

Matt Torrico
mtorrico@utk.edu

Matthew N. Torrico
The University of Tennessee, mtorrico@utk.edu

Recommended Citation

PP and CNO-Cycle Nucleosynthesis: Kinetics and Numerical Modeling of Competitive Fusion Processes

M.N. Torrico[A], M.W. Guidry[A,B]

[A] *Department of Physics and Astronomy, University of Tennessee, Knoxville, TN 37996, USA*

[B] *Physics Division, Oak Ridge National Laboratory, Oak Ridge, TN 37831, USA*

Signed on 21 April 2012

Abstract

The very history of matter (and hence Man) is exquisitely coupled to the nuclear fusion processes that power the Sun and other stars. The fusion of hydrogen into helium and other thermonuclear fusion processes (collectively called *nucleosynthesis* processes) provides us with not only the energy to carry on our lives, but the very materials that constitute our very bodies and our world. Nuclear fusion, a 'green' energy-liberating process that has been at the forefront of cutting-edge scientific research for decades, is carried out continuously in the sun at scales so large that they dwarf the totality of all human experimentation into harvesting nuclear energy. This review paper summarizes the basic physics and nuclear science that allows this process to happen, and attempts to describe in some depth recent efforts to accurately simulate the kinetics of these pathways, and describe what can happen when different simultaneously-occurring fusion reactions compete to dominate isotope production in stars of varying mass.

Introduction and Statement of Purpose

Kinetics is (broadly speaking) a discipline of science concerned with the rates of various processes and how these rates qualitatively (and quantitatively) affect the processes as a whole. The reader already familiar with *reaction kinetics* has probably been exposed to the theory in the context of *chemical reactions*. For the purposes of this discussion we will be primarily concerned with the rates of *thermonuclear* (high-temperature) *fusion reactions*, such as the ones that occur in the Sun. The rates of these processes set a lower bound on how long the Sun can fuse hydrogen into helium—the very process that currently provides us with radiant heat and enriches the interstellar medium with heavy elements for future stellar and planetary development. Research by Kelvin, Helmholtz, and others in the late 19th century proved both observationally (the 'unknown' spectral lines of atomic helium and the radiocarbon dating of moon rocks) and theoretically that gravitational heating alone cannot provide the temperature *or* apparent longevity of the Sun and the solar system. The tumultuous development of quantum mechanics in the early 20th century, spurred in part by the revolutionary discoveries of Bohr, Rutherford, Curie, and others, and the birth of modern astronomical spectroscopy (developed at Harvard) helped to perpetuate a revolution in astrophysics that would do away with the inaccuracies of the *Kelvin-Helmholtz timescale* and give birth to a more accurate theory of stellar longevity: *the nuclear timescale*. This review does not seek to introduce the reader to all of the aforementioned subjects (references to more comprehensive texts are provided), but rather strives to describe (in as little detail is as possible without loss of precision) the foundations of nuclear astrophysics and its implications.

Requisite Concepts from Nuclear Physics

Consider the nuclear two-body reaction:

$$A + B \rightarrow X^* \rightarrow C + D \qquad (1)$$

where X* represents the excited transition state (reaction intermediate) of the reaction (a 'compound state nucleus' in the words of N. Bohr). We will be primarily concerned with the *rates* of reaction for incident particles (*entrance channel*) A+B and products (*exit channel*) C+D.

The reader may recall from elementary physics that weakly interacting gas particles have velocities described by the *Maxwell-Boltzmann Distribution of Speeds*:

$$n_v \, d^3v = n \left(\frac{m}{2\pi kT} \right)^{3/2} \exp\left(\frac{mv^2}{2kT} \right) 4\pi v^2 dv \qquad (2)$$

where n particles are assumed to occupy a range of velocities between v and v+dv, and d^3v represents the differential volume element in a 3-dimensional space. For the sake of clarity this discussion will favor center-of-mass coordinates, meaning the following substitutions become useful:

$$E = \frac{1}{2}\mu v^2 = \frac{1}{2}\frac{m_A m_B}{m_A + m_B} v^2$$

where μ represents the *reduced mass* of entrance channel particles A+B. These substitutions allow (2) to be rewritten in a more convenient form that conveys energy dependence:

$$n_E \, dE = \frac{2n}{\sqrt{\pi}} \frac{\sqrt{E}}{(kT)^{3/2}} \exp\left(\frac{-E}{kT} \right) dE \qquad (3)$$

now taken as a distribution in energy space. Equation (3) gives the number of nuclei per unit volume with energies between E and E+dE, but does not specify *whether these nuclei will ineract*. To this end we introduce the concept of the *nuclear cross section.* For our reaction (1), the cross section is defined as

$$\sigma = \frac{\# \, reactions/target/time}{\# \, incident \, nuclei/area/time} = \frac{\rho_{AB}}{F(E)} \qquad (4)$$

where ρ_{AB} represents the density of reactions per target nucleus and F(E) represents the flux of incoming nuclei with energy E. Nuclear cross sections are typically measured in barns, where 1 barn = 100 square femtometers). For the present discussion we will adhere to the cgs system of units.

In order to determine a usable form of (4) we must average over all possible kinetic energies, which allows $\sigma(E) = \langle A,B \rangle$, the energy-integrated cross section of the reaction between projectile nucleus A and target nucleus B, to be put into an explicit integral form:

$$\langle A,B \rangle = \sqrt{\frac{8}{\pi\mu}} (kT)^{-3/2} \int_0^\infty E\sigma(E) \exp\left(\frac{-E}{kT} \right) dE$$

$$(5)$$

The full mathematical treatment of where (5) originates will be relegated to Appendix I. To be brief, (5) is obtained when one integrates the product of the energy distribution with the nuclear cross-section. We may now construct a general equation for the rate of reaction of projectile nucleus A with target nucleus B:

$$r = N_A N_B \langle A, B \rangle \quad (cm^{-3} s^{-1}).$$

(6)

It should not be surprising to the reader that most of the relevant thermonuclear reactions studied in astrophysics are exothermic; the energy of particles in the exit channel is much greater than in the entrance channel (if the converse of this statement were true, perhaps there would be no humans alive today to discuss it!). The exothermic nature of reactions in the form of (1) allows us to temporarily ignore the rather complex issue of *resonances.* Resonances in nuclear reactions occur when the compound nucleus X* (the reaction *intermediate*) exists in a quasibound state of similar energy to the *center of mass energy* of the entrance channel. The physics behind these resonances are beyond the scope of this paper but as previously mentioned we may partly ignore these complications and treat the cross sections in (5) as nonresonant. Another complication that may alter the mathematical form of (5) is the fact that in astrophysical plasmas (e.g. the Sun and other stars) not all nuclei are in their ground states. The atomic nucleus, like the atom itself, is not a 'soup' of subatomic particles but rather exhibits complex quantized structure of its own. The modern theory of the nucleus, called the *nuclear shell model* (much in the same way that electron orbitals are often grouped into 'shells' according to their principal quantum number, n), was developed concurrently with the modern wave-mechanical model of the atom championed by the likes of Linus Pauling and Paul Dirac. The nuclear shell model stipulates that nuclear structure is quantized by the same physical parameters that appear in the modern atomic theory, such as angular momentum and energy. While an in-depth discussion of nuclear structure goes beyond the scope of this paper, the interested reader may refer to both [2] and [9].

Coulombic Repulsion and Quantum Tunneling

The relative rarity of some fusion processes in the Sun (to be examined in a later section) may be attributed to the electrostatic (*Coulombic*) repulsion that exists between two positively charged helium

nuclei. The nuclei must tunnel through a Coulombic potential on the order of

$$V \sim \frac{Z_A Z_B e^2}{4\pi\varepsilon_0 R}$$

(6)

where Z_A and Z_B are the charges of nuclei A and B in terms of the fundamental electric charge e (measured in Coulombs), and an internuclear separation R (a measure of distance, given in femtometers). From the laws of classical physics, it can be shown that the mean proton temperature needed to overcome a Coulombic barrier of energy V is then given by

$$\frac{3}{2} kT = \frac{Z_A Z_B e^2}{4\pi\varepsilon_0 R}$$

$$\therefore T = \frac{Z_A Z_B e^2}{6k\pi\varepsilon_0 R}$$

for T the *classically*-approximated proton temperature. Assuming the radius of a typical hydrogen-1 nucleus is approximately 1 femtometer, this would require a classical temperature of $T \sim 10^{10}$ K, which is over *one thousand times hotter* than the core of the sun. It would seem improbable that any such reaction could occur under such unfavorable circumstances, but this is where the reader must remember that our expressions have been derived *classically* without any regard to the complex (and oftentimes, surprising) nature of quantum mechanics. One quantum phenomena in particular that we (quite literally) owe our very existence to is *quantum tunneling*, often referred to in the physics literature as *barrier penetration*.
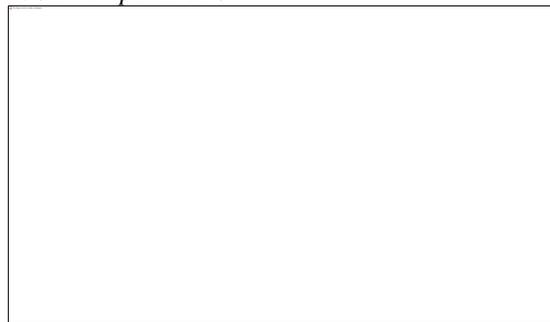

Figure 1: The coulomb barrier for a simple two-body charged particle reaction. Image reproduced with permission from [3].

Quantum tunneling asserts that a classically-forbidden potential energy barrier (or *wall*) between two charged particles may be 'tunneled' through if the distance between the two (indistinguishable)

particles is on the order of the *de-Broglie wavelength* of the particle. For the present discussion let us assume that the entrance channel particles that will be considered for fusion are protons (as is the case in the Sun). Figure 1 shows that protons repel one another unless a sufficient pressure gradient exists such that the protons may approach within one de-Broglie wavelength of one another. At this point the *strong nuclear force* interrupts the Coulombic repulsion and allows for fusion to take place. The strong nuclear force (often referred to simply as the 'strong force) is the strongest of the four fundamental forces of nature (strong, weak, electromagnetic, gravitation) but only operates on length scales characteristic of the de Broglie wavelength. Hence only the extreme temperatures and pressures of a stellar core are suitable for proton-proton fusion—anything less dense or less hot and fusion simply cannot occur due to Coulombic repulsion (this has important implications as to the explanation of pre-stellar mass objects observed in recent years known as *brown dwarfs* that appear too cold and not massive enough to fuse hydrogen).

Quantum tunneling allows for this conundrum to be resolved by rewriting the kinetic energy kT in terms of the de Broglie momentum, $p=h/\lambda$. It may then be shown that the temperature allowed by quantum tunneling becomes

$$T_{\text{quan}} = \frac{Z_A^2 Z_B^2 e^4 \mu}{12\pi^2 \varepsilon_o^2 h^2 k} \qquad (7)$$

where mean molecular weight $\mu=m(proton)/2$ and all nuclear charges are presumed to equal unity. Solving (7) gives a classically-forbidden temperature $\sim 10^7$K. This is consistent with the observed (and theoretical) core temperature of the sun. Another factor that may affect barrier penetration is *electron screening*, which is intuitively conceptualized as a 'decrease' in Coulombic repulsion due to the background 'sea' of electrons present in high-temperature plasmas. Two positively charged particles will experience less repulsion when 'dissolved' in this sea of electrons than in a hypothetical plasma of 0% ionization. Electron screening may be dealt with mathematically by introducing another energy term that depends on the internuclear separation:

$$V \sim \frac{Z_A Z_B e^2}{4\pi\varepsilon_o R} + V_{\text{scr}}$$

where V_{scr} represents the electron-screening contribution to the repulsive energy.

The Gamow Window

Let us assume that the energy of the Coulombic barrier is much greater than the thermal energy of the core protons $\left(E_{clb} >> E \right)$. Then the probability for a tunneling event to occur (all velocities up to this point are assumed to be nonrelativistic) is given by $P(E) \sim \exp(-2\pi\eta)$ where η is the *dimensionless Sommerfield parameter:*

$$\eta = \frac{\sqrt{\mu}}{2} \frac{Z_A Z_B e^2}{\hbar\sqrt{E}} \qquad (8).$$

This quantity contains information on proton masses, charges, and energies relevant to a fusion reaction. It is a convenient quantity for the parameterization of the energy-integrated cross section $\sigma(E)$, as it seems clear to us at this point that $\sigma(E)$ is somehow dependent on the probability of a tunneling event given by P(E). Combining P(E) and $\sigma(E)$ requires the introduction of a new quantity, the *astrophysical S-factor*, S(E), which gives the commonly cited relationship

$$\sigma(E) = \frac{S(E)}{E} \exp(-2\pi\eta) \qquad (9).$$

For the present discussion it will be assumed that S(E) is some function that varies <u>weakly</u> with the thermal energy of the protons, E. With the assistance of the S-factor and the Sommerfield parameter, some algebraic manipulation allows equation (5) to be re-written as

$$\langle A,B \rangle = \sqrt{\frac{8}{\pi\mu}} (kT)^{-3/2} \int_o^\infty S(E) e^{-E/kT} e^{-b/\sqrt{E}} dE \qquad (10)$$

where $b = 2\pi\sqrt{\mu/2} Z_A Z_B e^2/\hbar$ (essentially a collection of constant terms pertaining to the probability of a quantum tunneling event). Hence the energy-dependence of (10) lies primarily in the product $e^{-E/kT} e^{-b/\sqrt{E}}$, which is termed the *Gamow window*, after George Gamow, the physicist who first recognized its astrophysical importance. While perhaps not immediately obvious, the very likelihood of the solar fusion reactions to which we owe our very existence may be found in this (temperature-dependent) Gamow window. The reason it is called a 'window' will be made clear to the reader who understands figure X. To the left of the Gamow window we have sufficient $e^{-E/kT}$ but insufficient probability for barrier penetration (
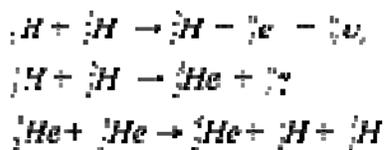
$e^{...} \rightarrow]$ *as* $b \rightarrow []$). To the right of the Gamow window there is significant probability for barrier penetration, but the kinetic energy (as quoted from the velocity distribution) is too high for fusion. Only *within the Gamow window* can particle collisions occur with significant probability for fusion.

Figure 2: Only those reactions with energies that lie within the Gamow window have significant probability of occurring. Image reproduced from [3].

PP Chain and CNO Cycle Nucleosynthesis

The energy output of the sun is dominated by the **proton-proton chain reaction** (henceforth the PP chain), which provides the heat necessary to maintain a habitable Earth. The PP chain is also arguably the simplest nucleosynthesis process but does not enrich the interstellar space with any metallic elements, as it involves mainly the formation of helium-4. The principle reactions occurring during proton-proton nucleosynthesis (AKA 'hydrogen burning') are given as follows:

$$_1^1H + _1^1H \rightarrow _1^2H + _1^0e + _0^0\nu$$
$$_1^2H + _1^1H \rightarrow _2^3He + \gamma$$
$$_2^3He + _2^3He \rightarrow _2^4He + _1^1H + _1^1H$$

Reaction 1: The PPI Chain.

which accounts for approximately 69% of the solar helium-4 production. This is the **PPI** chain. Another branch of the PP chain (called the **PP II** chain) accounts for another 30% of the solar helium production:

$$_2^3He + _2^4He \rightarrow _4^7Be + \gamma$$
$$_4^7Be + _{-1}^0e \rightarrow _3^7Li + \nu$$
$$_3^7Li + _1^1H \rightarrow _2^4He + _2^4He$$
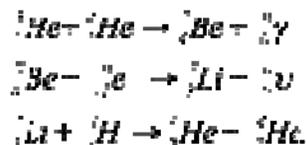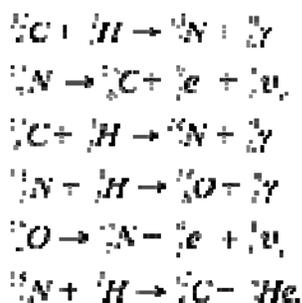
Reaction 2: The PPII Chain.

The relative rarity of this process may be attributed to the electrostatic (Coulombic) repulsion that exists between two positively charged helium nuclei. Rarer still than the PP II chain is the **PP III** chain, which may represent ~1% of solar proton-proton nucleosynthesis:

$$_4^7Be + _1^1H \rightarrow _5^8B + \gamma$$
$$_5^8B \rightarrow _4^8Be + _1^0e + _0^0\nu$$
$$_4^8Be \rightarrow _2^4He + _2^4He$$
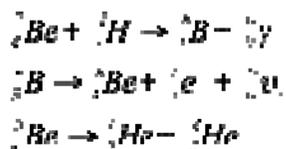
Reaction 3: The PPIII Chain.

The reader may verify that a similar argument involving quantum tunneling illustrates that the core solar temperature is sufficient, but low, for PP III nucleosynthesis to occur. However, the extreme rarity of the PP III chain is actually attributed to the improbability of proton capture by a beryllium nucleus when there are plenty of electrons around for PP II fusion to take precedence.

The other nucleosynthesis process to be discussed here is the CNO (carbon-nitrogen-oxygen) cycle, which is strongly temperature-dependent and occurs in hotter, more massive stars. The primary CNO reactions involve the consumption and subsequent *catalytic regeneration* of carbon-12:

$$_6^{12}C + _1^1H \rightarrow _7^{13}N + \gamma$$
$$_7^{13}N \rightarrow _6^{13}C + _1^0e + _0^0\nu$$
$$_6^{13}C + _1^1H \rightarrow _7^{14}N + \gamma$$
$$_7^{14}N + _1^1H \rightarrow _8^{15}O + \gamma$$
$$_8^{15}O \rightarrow _7^{15}N + _1^0e + _0^0\nu$$
$$_7^{15}N + _1^1H \rightarrow _6^{12}C + _2^4He$$

Reaction 4: The reactions that account for ~99% of CNO nucleosynthesis.

The end product helium-4 is *not* catalytically regenerated, but rather is produced as a result of the proton capture reactions that take place in steps 1, 3, 4, and 6 in the overall cycle. This places an upper bound on how long CNO burning can last—as long as there is hydrogen and carbon present. It should also be noted that there is a second branch of the CNO cycle involving the formation of a fluorine-17 intermediate, but it is important in less than 1% of cases.
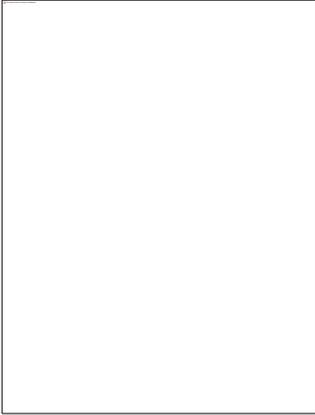
Figure 3: Diagrammatical representation of the CNO processes which more clearly shows its 'cyclic' nature. The notation (X,Y) means capture of X by an incident nucleus, followed by emission of Y.

Density and Temperature Dependence of Fusion Rates: Simulation and Results

While density and temperature dependence of the reaction rate is a complex topic, for nuclear reactions of astrophysical interest some generalities may be made that allows for easier discussion. Firstly it is useful for the sake of visualization to parameterize the nuclear energy production as a power law in both mass density (ρ) and temperature (T):

$$\zeta = \zeta_0 \rho^\lambda T^\upsilon \qquad (11)$$

where ζ represents the rate of energy output from fusion, λ is the density exponent, and υ is the temperature exponent (both exponents are assumed to be constant). These exponents may be isolated by differentiation:

$$\lambda = \left(\frac{\partial \ln \zeta}{\partial \ln \rho} \right)_T , \quad \upsilon = \left(\frac{\partial \ln \zeta}{\partial \ln T} \right)_\rho .$$

This power-law parameterization of the density/temperature dependence is not universally applicable, but for many simplified models of stellar modeling and the assumption of local thermal equilibrium (LTE) it may be invoked. Power law curve fitting to data for the combined PP and CNO processes yields temperature exponents of approximately 4 and 16, respectively (the exponent may even exceed ~40 for fusion processes in more massive stars). Both density exponents for the PP chain and the CNO cycle are found to be

unity. The extreme sensitivity of these processes to changes in temperature begs the question: to what extent must the temperature in the solar core be increased before energy production becomes dominated by CNO nucleosynthesis? How does this relate to the mass of the star?

To answer this question (and others), *ElementMaker,* a Java-based numerical modeling program for nuclear physics, was employed. *ElementMaker* (EM) uses a *quasi steady-state* approach for analysis of the systems of ordinary differential equations (ODEs) involved in thermonuclear rate laws. EM involves a graphical-user-interface resembling the chart of the nuclides, where atomic number is plotted along the y-axis and neutron number is plotted along the x-axis. The user selects relevant isotopes for the simulation, rate laws, and hydrodynamic variables (density, temperature, and mass fraction) before running the simulation. Figures 4-6 show some basic graphs produced in EM, with commentary. The basic plot shows the common log of abundance on the y-axis (with values ranging from -14 to 0) and log time on the x-axis. Each simulation was run under the assumption that hydrogen would be depleted before termination. Different colored lines represent the nuclides produced, and the total integrated energy produced during the process is also plotted as a dashed line. The hypothesis to be tested is that as the temperature increases for a given library of isotopes (all contained in a single file to be called upon by the program), the abundance of CNO-specific nuclides (such as oxygen-15) should increase, and the abundance of pp-chain-specific isotopes (such as beryllium-7) should decrease.
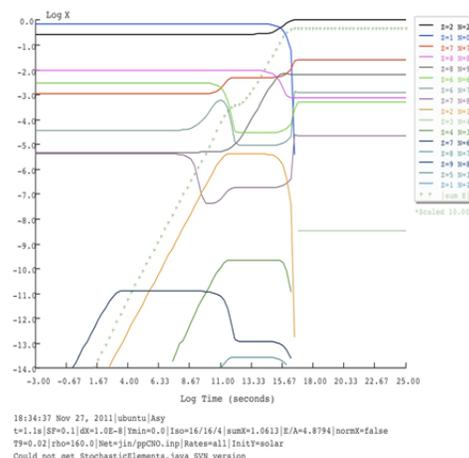

Figure 4: T~20 million Kelvin, rho=160 g per cc. Solar abundances assumed for all listed isotopes.

Figure 4 was prepared in order to analyze the isotopic production and competition between PP and CNO nucleosynthesis in a stellar core that is somewhat hotter than the sun, but of approximately the same density. The 4th-degree temperature dependence of the PP chain means that adjusting the temperature slightly should have a significant effect. Consider the Z=2 N=1 line, corresponding to helium-3: the production of helium-3 as an intermediate of PP nucleosynthesis means that once the helium-3 begins to deplete, another isotope should begin to manifest. In this case, the reaction

$$\frac{3}{2}He + \frac{3}{2}He \rightarrow \frac{4}{2}He + \frac{1}{1}H + \frac{1}{1}H$$

becomes important. The black helium-4 line (Z=2, N=2) near the top of the diagram (log X = -0.5) remains constant but begins to increase as the helium-3 begins to deplete. The 'slight' increase in the helium-4 line corresponds to a 'drop in the bucket,' as there is already such a high abundance of the isotope that its further formation will take a backseat to the other reactions that are occurring.
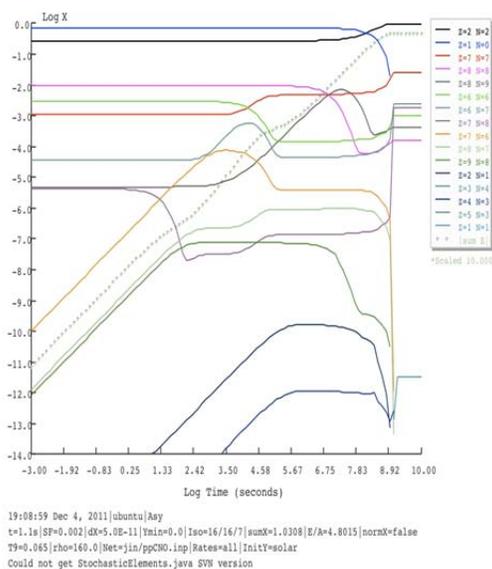

t=1.1s|SF=0.002|dX=5.0E-11|Ymin=0.0|Iso=16/16/7|sumX=1.0308|E/A=4.8015|normX=false
T9=0.065|rho=160.0|Net=jin/ppCNO.inp|Rates=all|InitY=solar
Could not get StochasticElements.java SVN version

Figure 5: T~ 65 million Kelvin, rho=160 g per cc. Solar abundances assumed for all listed isotopes.

Figure 5 considers a significantly hotter (by a factor of 3) stellar core where CNO nucleosynthesis becomes the prominent form of energy output. The reasoning for this is as follows: the CNO cycle does not involve the production of deuterium (hydrogen-2), which is shown in the legend as the Z=1 N=1 line. Indeed, this bright, cyan-colored line does not

appear on the graph, as it would if PP chain nucleosynthesis was dominant. Referring back to figure 4 shows that the line closest to the bottom of the diagram, which peaks at log t = 13.33 seconds, is the deuterium line. Even in the pp chain, deuterium is produced only in small amounts and should be subsequently consumed as

$$\frac{2}{1}H + \frac{1}{1}H \rightarrow \frac{3}{2}He + \gamma.$$ It is also worth noting that the total time accounted for on the diagram, 10^10 seconds, represents the nuclear fusion timescale for the hypothetical star. More massive, hotter, CNO-cycle stars should burn for a much shorter time span than a typical pp chain-burning star like our own sun.

Figure 6 should appear at least somewhat similar to the empirically derived abundance curves for solar fusion. The chosen temperature and density were chosen specifically because they are the sun's core temperature and density. Hydrogen burning appears to take place for 10^18 s (around 31 billion years), which is longer than the hydrogen burning timescale of the sun, but by less than an order of magnitude. Furthermore, the red Z=N=8 line corresponding to the oxygen-16 abundance remains constant, as it should considering that oxygen-16 is not produced during the pp chain.

t=2.1s|SF=0.1|dX=5.0E-10|Ymin=0.0|Iso=16/16/7|sumX=1.0840|E/A=5.0757|normX=false
T9=0.012|rho=160.0|Net=jin/ppCNO.inp|Rates=all|InitY=solar
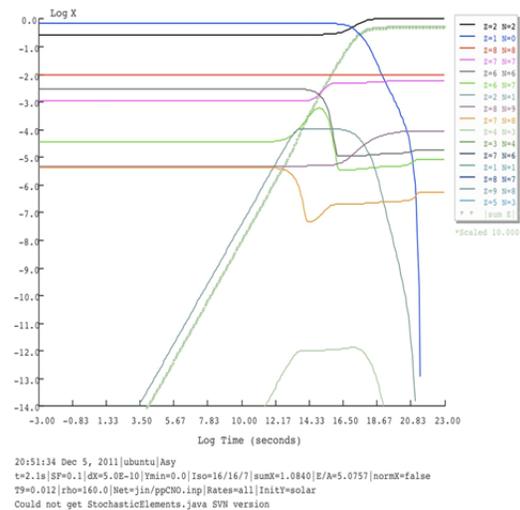Could not get StochasticElements.java SVN version

Figure 6: T~12 million Kelvin, rho=160 g per cc. This figure is more akin to what theoretical solar nucleosynthesis should look like. Notice the transient production of unstable beryllium-7.

Note also the dotted lines evident in fig. 4-6, which represent the *total integrated* energy production for the process over the entire time interval for the calculation. One may logically establish that the

rate of energy output may be plotted against a thermodynamic variable that characterizes the star under investigation. Indeed, plotting rate of energy production vs. temperature produces a plot that indicates clearly the "turn on" and "turn off" points for PP and CNO nucleosynthesis, and it just so happens that our very own Sun lies near the temperature at which energy production via CNO burning should take dominance: the competittion between these nucleosynthesis processes is truly a war waged with temperatures (figure 7).
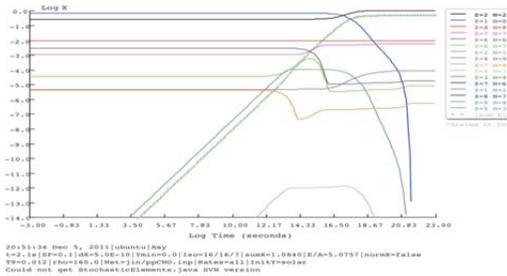

Figure 7: log(rate of energy production) plotted against temperature, where T(6) denotes units of one million Kelvin. Notice that the Sun lies near the upper-temperature limit for PP chain-dominated energy output.

Thermonuclear Reaction Networks: Theory

All reactions discussed up to this point can be functionally divided into three categories according to the number of reactant nuclei: single-body processes (decays, electron captures, photodisintegrations), two-body collisions, and three-body collisions. Three body reactions, although considerably rare, must be reckoned with due to their astrophysical interest and are typically viewed as subsequent two-body reactions via an unstable intermediate ('compound') nucleus. For example, the three-body reaction given by

$$^4_2He + ^4_2He + n \rightarrow ^9_4Be + \gamma$$ (where 'n' represents a thermal neutron) may be equivalently represented as a two-step reaction sequence

$$^4_2He + ^4_2He \rightarrow ^8_4Be^*$$
$$^8_4Be^* + n \rightarrow ^9_4Be$$
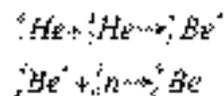
where (*) denotes a transient or unstable species. The convenient grouping of reactions into three simple classes allows for easier mathematical modeling (notice that up to this point no mention of reaction equilibrium has been made). Now consider

the rate of change (time derivative) of the *number density* of nucleus A. The relationship that describes the time evolution of the species is a differential equation:

$$\frac{dY_n}{dt} = F_n^{(+)}(\mathbf{Y}) - F_n^{(-)}(\mathbf{Y}) \tag{12}$$

where Y is the mass fraction of the nth isotope (more generally we would consider the *abundance* of the isotope, but defining the abundance is a delicate topic that is beyond the scope of this paper) and $\mathbf{Y}$ denotes a vector whose components are the possible abundances of n, that is,

$$\mathbf{Y} = \begin{pmatrix} Y_1 & Y_2 & \dots & Y_n \end{pmatrix}.$$

The notation $F_n^{(+)}(\mathbf{Y})$ indicates that the summation of all possible terms that increase (+) the abundance of the nth isotope be taken, and likewise $F_n^{(-)}(\mathbf{Y})$ denotes the summation of all terms that decrease (-) the abundance of the nth isotope. This is the simplest possible way of denoting what is otherwise a rather cumbersome set of equations. Because there are many isotopes that constitute realistic stellar plasmas, we end up with a system of nonlinear equations that fully describe the time evolution of our reaction network:

$$\dot{Y}_1 = F_1^{(+)}(\mathbf{Y}) - F_1^{(-)}(\mathbf{Y})$$
$$\dot{Y}_2 = F_2^{(+)}(\mathbf{Y}) - F_2^{(-)}(\mathbf{Y})$$
$$\vdots$$
$$\dot{Y}_n = F_n^{(+)}(\mathbf{Y}) - F_n^{(-)}(\mathbf{Y}) \tag{13}$$

Even the simplest thermonuclear network cannot be solved analytically, and for realistic plasmas we may encounter upwards of 100 isotopes. Only with the advent of modern computing can these systems be accurately modeled. Non-trivial complexities arise when considering the overall time evolution of a many-isotope system. Because fusion reactions in a realistic plasma occur amid a background of high-energy photons, *photodisintegrations* are possible that decompose heavier nuclides into lighter ones, e.g.,

$$^{14}_7N + \gamma \rightarrow ^{14}_7N^* \rightarrow ^{13}_7N + n$$

Reaction 5: One of the simplest photodisintegrations that can occur in stars. Photodisintegrations are endothermic.

The excited-state nucleus $_1^2H^*$ is the unstable intermediate that then rapidly decays into hydrogen-1 and a thermal neutron. When the target B in equation (5) is a photon rather than a nucleus then we must integrate over the Planck distribution,

$$B_\lambda(T) = \frac{2hc^2}{\lambda^5} \frac{1}{\exp\left(\frac{hc}{\lambda kT}\right) - 1} \quad (14)$$

where the notation $B_\lambda(T)$ indicates the distribution is expressed in terms of wavelength λ and is temperature-dependent. Photodisintegrations are highly endothermic and require gamma rays in the high-energy tail of the Planck spectrum. It seems logical then to surmise that photodisintegrations become most important in the deep stellar interior.

Another consideration is that of equilibrium. The primary condition for equilibrium is that the *timescale for equilibration* must be shorter than other relevant timescales of competition. For example, the reaction $i + j \rightarrow k + l$ will rapidly approach equilibrium if the rate of the reverse reaction $k + l \rightarrow i + j$ is at least as rapid as other relevant hydrodynamical timescales. For interacting particles described by a Maxwell-Boltzmann distribution (2) the critical parameter that will affect equilibrium is the temperature, T (as a heuristic, many chemists apply the rule that for every ten degree increase in T, the rate of reaction doubles). For stellar cores of sufficient temperature and density (prescribed by the stellar mass) such equilibria may become a crucial ingredient in achieving computational results that match observation. While this complication will not strongly impact the present discussion, as a heuristic it would seem that reactions involving the weak force (beta decays) are *least* susceptible to equilibration under the conditions present in most PP and CNO-burning stellar cores. For more on the subject of chemical and nuclear equilibrium in astrophysics, see [1].

Nuclear Reaction Networks: Numerical Modeling and Instability

The accurate simulation of even 'boring' main-sequence stellar fusion processes involve mathematics convoluted enough to preclude high-level modeling before recent advances in computational science and supercomputing made them feasible. A high-end desktop PC from 2000 or 2005 can model basic thermonuclear kinetics and isotope production (as represented in fig. 4-6) for reasonably large reaction networks efficiently (assuming the *integration timestep* is large enough such that the computer will not become bogged down in computation). The coupled set of nonlinear ODEs in equation (13) is the simplest set of such equations that can model even a hypothetical stellar core, and this ignores completely the subject of hydrodynamics. Thermonuclear reactions generate energy that will be absorbed (or scattered) by the bulk medium, influencing the properties of the fluid. We have assumed for the sake of simplicity that the hydrodynamics may be sufficiently decoupled from the rest of the system. The interested reader may refer to [2].

One complication that makes solving even hydrodynamically-decoupled reaction networks a tedious and sensitive process is that of *numerical instability* and *stiffness*. The former will be manifest in the latter. A set of *stiff* differential equations may be practically defined as ones that depend on many timescales that differ by orders of magnitude. For example, the first proton capture reaction of the PP chain, $_1^1H + _1^1H \rightarrow _1^2H + e^+ + \nu_e$, has a mean timescale of $\tau \sim 10^{10}\,yr$, while the reaction immediately following it, $_1^2H + _1^1H \rightarrow _2^3He + \gamma$, has a timescale of only a few seconds. Thus, the difference in timescales between the two successive PPI reactions is over <u>fifteen</u> orders of magnitude, and the resulting reaction network is extraordinarily stiff. The solution of a *stiff reaction network* will lead to numerical instability unless the *integration timestep* (the time difference taken by the computer between successive numerical integrations) is sufficiently small. However, with decreasing step size comes increasing computational cost. A basic calculation of the type employed in producing figure 4 running on a desktop PC, *decoupled* to hydrodynamics, and using an integration timestep small enough to prevent the production of 'garbage numerics,' would take longer than the age of the universe (13.5 billion years) to complete. Obviously such methods have been abandoned in favor of more shrewd algorithms such as *implicit* and/or *explicit temporal integration*, which makes use of the finite difference operator in calculating derivatives. Consider for an arbitrary isotopic abundance Y the finite difference equation

$$\frac{dY}{dt} = \frac{Y(t + \delta t) - Y(t)}{\delta t} \quad (15)$$

for δt representing a small (but measurable) time interval. This is the *integration timestep*. Taking the limit of (15) as t→0 turns the equation into a derivative, but the arbitrary choice of δt is what makes the method of finite differences work. Iterating the prescription outlined by (15) until a qualitatively accurate solution is obtained is known as the *Forward Euler* Method for solving systems of ODEs. A Taylor expansion about t returns f(t), the *explicitly-evaluated* finite difference. Because the Taylor series used in approximating f(t) must be truncated, the resulting equations may or may not be accurate to a first approximation (this is the *local truncation error*). Accuracy is sometimes a function of the number of iterations taken before truncation, but in the case of a stiff system instabilities may arise: even judicious use of the Forward Euler Method (FEM) can produce solutions that tend to infinity during 'small' timesteps when the correct analytical solution should not. When these reaction networks are coupled to hydrodynamics, multivariable instabilities such as solitons may result. See [8].

Ultimately we seek to numerically integrate the finite difference and apply the fundamental theorem of calculus:

$$Y(t + \delta t) - Y(t) = \int_{t}^{t + \delta t} f(t, Y(t)) dt.$$

These integrals are typically calculated using a modified trapezoidal algorithm such as Simpson's Rule. Successive iterations can be numerically hazardous because of numerical instability, or because one has chosen a step size too small to be practically applicable. Both issues are one and the same. What if instead we were to make a Taylor expansion of (15) about f(t+δt)? This means we are evaluating f at some *later time* represented by t+δt. This is the *Reverse (or Implicit) Euler Method* (REM). The correct choice of FEM or REM for practical simulation of a particular reaction network is very sensitive to certain physical conditions (namely temperature and density) and the discussion will hence be relegated to a more advanced source (see [1] or [2]). However, for the calculations *ElementMaker* performed on CNO and PP burning stars, a *quasi-steady-state* solver proves convenient for the (relatively) small isotope libraries characteristic of these stars. *Steady-state* refers to the idealized situation in which all time derivatives of concentration are exactly zero. In general, steady-state allows for a complex set of differential equations (equation 13) to be reduced to a set of simple *algebraic* equations, that can be

solved via matrix inversion (see [1]). The detailed mathematics behind matrix solutions is beyond the scope of this review.

Further Research

The accurate modeling of even main-sequence stellar evolution requires the aforementioned numerical complexities inherent in many-body nuclear systems, coupled to hydrodynamics. Recent investigations at Oak Ridge National Laboratory (ORNL) into the large-scale structure of stars modeled using the assumptions detailed in this review have yielded impressive visual demonstrations of what modern computing is capable of. The recent addition of *Jaguar* to ORNL's armory of computational power means that even the extremes of stellar evolution, including degenerate remnants of massive stars (neutron stars, etc.) may soon be within the reach of theoretical modeling.

Acknowledgements

References

1) Hix, W.R. and Meyer, B.S. "Thermonuclear kinetics in astrophysics." *Nucl. Phys. A.* 777 (2006) 188-207.
2) Arnett, David. *Supernovae and Nucleosynthesis: An Investigation of the History of Matter, from the Big Bang to the Present.* Princeton University Press, 1996.
3) Guidry, Mike. *An Introduction to Stars, Stellar Evolution, and Galaxies.* In press.
4) Ryan, S.G. and Norton, A.J. *Stellar Evolution and Nucleosynthesis.* Cambridge University Press, 2010.
5) Adelberger, E.G. *et al.* "Solar fusion cross.. II." *Rev. Mod. Phys* 83 (2011) 195.
6) Carroll, B.W. and Ostlie, D.A. *An Introduction to Modern Astrophysics, 2nd Edition.* Addison-Wesley, 2007.
7) Lewis, John. *Physics and Chemistry of the Solar System, Rev. Ed.* Academic Press, 1997.
8) Strauss, Walter. *Partial Differential Equations, 2nd Ed.* Wiley, 2008.

9) Kaplan, Irving. *Nuclear Physics, 2nd Ed.* Addison-Wesley, 1964.

Appendix I: Derivation of the Thermally-Averaged Cross Section

We begin with the most basic assumption of local thermodynamic equilibrium: the mathematics associated with stellar structure are greatly simplified by assuming thermodynamic equilibrium. For most astrophysical plasmas the ideal gas equation of state is valid to a first approximation:

$$PV = NkT \qquad \text{(A1).}$$

For mean molecular weight μ we have the following expressions, all equivalent to (A1):

$$P = \rho kT = \frac{Nm_H}{V} RT = \rho \frac{kT}{\mu m_u}$$

where m_u is the approximate mass of a hydrogen nucleus, ρ is the mass density, and R is the commonly-encountered gas constant which depends on the unit of pressure (often approximately equal to 8.314 J/(mol*K)). For the general 2-body reaction involving entrance channel nuclei A and B we have the Maxwell distribution of velocities

$$\Psi(E) = n \left(\frac{m}{2\pi kT} \right)^{\frac{3}{2}} \exp\left(\frac{-mv^2}{2kT} \right) 4\pi v^2 \qquad \text{(A2).}$$

In equation A2, (n) represents the number of nuclei of type A, and it is assumed that nuclei of type B have a similar velocity distribution. It is worth noting that the rare but non-negligible probability of an n-body collision (n>2) may be dealt with by assuming that all n-body reactions perpetuate as series of 2-body reactions. The familiar equation for the thermally-averaged reaction cross section, usually written as $\langle A,B \rangle$ for reaction between A and B, is then obtained by integrating the product of the cross section and the velocity distribution:

$$\langle A,B \rangle N_A N_B = \int \int \sigma(E) \Psi(E) d^3 N_A d^3 N_B. \qquad \text{(A3)}$$

Upon further substitution into (A3),

$$\langle A,B \rangle = \int \int \sigma(E) v \left(\frac{\mu}{2\pi kT} \right) e^{-\phi} d^3 v_A d^3 v_B$$

where the exponential factor contains the sum of the mass elements of the distribution:

$$\phi = \frac{(v_A^2 + v_B^2)}{2kT} \mu.$$

The differential volume element $d^3 X$ must be converted to something more readily integrable, and this is accomplished via sagacious use of the Jacobian determinant (see [2]). Upon back-substituting the standard equation for the kinetic energy we finally obtain the familiar equation for the thermally-averaged cross section

$$\langle A,B \rangle = \sqrt{\frac{8}{\pi \mu}} (kT)^{-3/2} \int_0^\infty \sigma(E) e^{-E/kT} E dE$$

which is equation (5).